ARCHIVES
of
FOUNDRY ENGINEERING

ISSN (2299-2944)
Volume 2025
Issue 4/2025

54 – 62

8/4

10.24425/afe.2025.155380

Published quarterly as the organ of the Foundry Commission of the Polish Academy of Sciences

A Study of the Mechanical Properties of Conventional and Additive Mould Parts for Die Casting of Aluminum Alloys

M. Pinta [a, b], L. Socha [a], J. Sviželová [a, *], L. Kucerova [b], M. Dvořák [c], J. Häusler [d]

[a] Department of Applied Technologies and Materials Research, Institute of Technology and Business in České Budějovice, Okružní 517/10, 370 01 České Budějovice, Czech Republic

[b] Department of Materials and Engineering Metallurgy, Faculty of Mechanical Engineering, University of West Bohemia, Univerzitní 2732/8, 301 00 Plzeň, Czech Republic

[c] Tool Shop Division, MOTOR JIKOV Fostron a.s., Kněžskodvorská 2277, 370 04 České Budějovice, Czech Republic

[d] MOTOR JIKOV Strojírenská a.s., Zátkova 495, 392 01 Soběslav II, Czech Republic

* Corresponding author: e-mail: svizelova@mail.vstecb.cz

Received 24.04.25; accepted in revised form 30.06.25; available online 22.12.2025

Abstract

The article focuses on the mechanical properties of mould parts created using 3D printing technology, for use in the production of castings by High-Pressure Die Casting (HPDC). The mould shapes produced by 3D printing technology bring innovative approaches to optimising production processes. H13 tool steel is widely used for its excellent mechanical properties and resistance to thermal stress. The study focuses on the comparison of the mechanical properties of mould parts produced by traditional methods and 3D printing, with emphasis on their strength, hardness and wear resistance under repeated working cycles. The experimental part includes roughness measurements and tests of mechanical properties, which provide important data on the ability of these components to withstand high mechanical loads and temperature fluctuations during the HPDC process. The results of the study show the advantages and limitations of 3D printing compared to traditional manufacturing processes and give insight into the use of additive technologies in industrial manufacturing. Specifically, the study identified clear quantitative differences in mechanical properties: the 3D printed mould parts had comparable ultimate tensile strength and yield strength to conventionally manufactured parts, but significantly lower ductility (below 1% compared to about 20% in traditional parts) due to higher porosity (0.25–0.30% compared to 0.03–0.04%). Additive mould parts exhibited higher hardness (approximately 510 HV) compared to conventional parts (approximately 450 HV). Surface roughness of the 3D printed parts was more variable, highlighting the need for optimising printing parameters. Thus, additive technology offers benefits in stable hardness and comparable strength, albeit at the expense of reduced ductility and increased variability in surface quality. The research also includes an analysis of the effect of repetitive loading on the mechanical properties of the mould parts made of H13, which provides valuable information for improving their durability and reliability in practice. This research contributes to the development of 3D printing technologies in the field of HPDC and offers new opportunities for improving the efficiency and quality of manufacturing processes in industrial applications.

Keywords: Mechanical properties, Tool steel, H13, 3D printing, HPDC

1. Introduction

Selective Laser Melting (SLM) is an advanced state-of-the-art technology for manufacturing components with minimal porosity, leading to improved mechanical properties and strength of a material under static and dynamic loading. Porosity decreases with increasing energy density (VED), while the hardness of the AISI H13 material increases. Energy density must be set correctly in order to achieve satisfactory mechanical properties [1]. SLM technology produces H13 steel components with a tensile strength of about 1900 MPa, yield strength of 1500 MPa, ductility of 6-10% and hardness of 540-570 HV. These properties are due to the fine microstructure created during the SLM process. SLM at a printing speed of 200 mm/s leads to optimum mechanical properties, including the highest hardness values when compared to lower or higher printing speeds [2]. Porosity in additively manufactured components adversely affects their mechanical properties, especially the material's fatigue resistance. The optimisation of 3D printing and post-processing parameters are crucial for the production of high quality parts [3]. H13 steel produced using SLM technology has a tensile strength of 513 MPa, whereas the conventionally manufactured H13 material reaches 659 MPa. No heat treatment was applied to any of the samples. Furthermore, additive H13 has a significantly lower ductility of less than 1% compared to the conventional material, which has a ductility of 21%, leading to brittle fracture. The hardness of the additively manufactured material averages around 450 HV, while the conventional samples show an average of 218 HV. This difference may be due to different heat treatment processes, such as annealing [4]. The H13 steel produced by the SLM technology achieves a tensile strength of 1837 MPa and a ductility of 8.5% due to the hierarchical microstructure containing martensite as the base matrix. Residual austenite (6-9%) and 500 nm cell structures contribute to grain hardening and increased resistance to deformation [5]. The samples are manufactured at a printing speed of 800 mm/s and a laser power of 200 W. The higher proportion of residual austenite in these samples can lead deformation-induced martensitic transformation. This phenomenon contributes to the material's ability to harden during deformation, thus improving its mechanical properties [6]. In the porosity analysis for H13 steel, a lower porosity with a value of 0.4% was observed in the middle of the samples. This porosity was found in samples produced at 800 mm/s with a laser power of 230 W. The defects discovered may further accelerate crack propagation [7]. Porosity is a key aspect affecting the mechanical properties of components produced by additive manufacturing [8]. Pores can form during the melting and solidification process of the powder, and their occurrence has a direct effect on the strength, hardness and durability of the components [9]. Targeted control of the microstructure around the pores during printing with SLM technology can partially compensate for the negative effect of porosity on mechanical properties. This can be achieved, for instance, by creating harder phases using rapid cooling [10]. Another important factor is surface roughness, also closely related to the SLM manufacturing technology. In additive manufacturing, uneven material melting and cooling occurs, potentially producing a rougher surface, about 6 to 12 μm, than traditional machining methods (e.g. CNC machining) where roughness values are <1 μm depending on the technology. Surface roughness plays a key role in evaluating wear, fatigue resistance and surface quality [11]. In combination with the presence of pores, further deterioration of the mechanical properties may occur, requiring detailed analysis and optimisation of process parameters [12]. Important process parameters include printing speed, laser power and construction orientation. These parameters have a direct impact on the resulting porosity and surface roughness. The right combination of printing speed, laser power and construction orientation minimises porosity and produces a smoother surface. For example, a lower printing speed with optimal laser power and vertical the part construction orientation generally delivers higher quality [13]. Effective control of printing speed, laser power and construction orientation in the SLM technology allows porosity to be reduced to below 0.5%, achieving surface roughness below 10 μm and improving the mechanical properties of H13 tool steel, which significantly increases its usability in industrial applications, such as for the production of moulds and tools with high wear resistance [14].

State-of-the-art a 3D metal printing technologies are starting to be used in the production of mould components as part of the trend towards modernisation and increasing competition in this field, giving rise to new knowledge and possibilities of high-pressure die casting that cannot be achieved by traditional production technologies. This includes, for instance, the ability to create complex structures and conformal cooling channels. This paper describes methods used to analyse components after operational testing in the die-casting plant of MOTOR JIKOV Slévárna a.s. The aim of applying additively manufactured mould parts was to replace conventionally manufactured components with additively manufactured components. Additive technology offers several advantages, such as the possibility of lightweight components to save material. Within this paper, additively and conventionally manufactured components are analysed and compared, with a focus on their mechanical properties. The analyses use evaluation methods such as microtensile testing, microhardness, surface roughness, microstructure determination, and porosity measurements.

2. Solution methods

The components were produced in cooperation with MOTOR JIKOV Fostron a.s (MJF) and three universities - University of West Bohemia (UWB), Technical University in Liberec (TUL) and University of Technology and Economics in České Budějovice (UTE). MJF designed and produced the components in cooperation with TUL using additive SLM technology. The material analyses, which are the focus of this paper, were performed at UWB. The methods for testing the selected components are described in the following sections.

2.1. Testing methods

The components were tested under operational conditions at the MOTOR JIKOV Slévárna a.s. die casting plant. The testing involved their deployment in a mould for die casting of aluminium alloys, where the expected lifetime was 120,000 casting cycles. The testing was performed on Colosio PFO1000 die-casting machines

with a maximum locking force of 9810 kN and a maximum injection force of 738 kN.
The designations of the alloys, their chemical compositions, and recommended casting temperatures are as follows:

- **AL 226 (AlSi9Cu3)**: approximately **680–720 °C**

Table 1.
Chemical composition AlSi9Cu3

Prvek %	**AL 226 AlSi9Cu3**
Al	zbytek
Si	8,0 – 11,0
Fe	1,3 max
Cu	2,0 – 4,0
Zn	1,2 max
Mg	0,05 – 0,55
Pb	0,35 max
Mn	0,55 max
Sn	0,25 max
Ni	0,55 max
Ti	0,25 max
Cd	x
Cr	0,15 max
Li	0,003 max
Be	0,02 max
Bi	0,05 max

After the operational testing of the components, the following analyses were performed:
- Porosity measurements
- Microtraction test
- Microhardness
- Surface roughness
- Microstructure determination

Porosity was measured using an Olympus LEXT OLS5000 laser confocal scanning microscope, which allows the detection of pores in the internal material structure. The size and shape of the pores can be quantified in the images obtained.

The tensile properties were determined by tensile testing on small samples performed on an MTS test machine. The strain rate was kept very low to avoid dynamic effects that could affect the results. The test speeds were controlled by the A1 method according to EN 6892-1. The testing was carried out under controlled environmental conditions at a constant temperature to minimise the effects of environmental factors on the material's mechanical properties. In this manner, yield strength, ultimate strength, ductility and elastic modulus were measured.

Vickers microhardness was measured on the UHL-VMHt-002V device. Due to the small impression size and the possibility of measuring diagonals under the microscope, this method is very accurate and enables the relevant values to be determined for comparing additive and conventional components.

Surface roughness was measured on the working part of the machine using an OLX 3000 confocal light microscope. This method enables an accurate assessment of material surface properties. The confocal microscope uses the optical sequence principle, where individual surface points are focused at different depths, making it possible to obtain a detailed three-dimensional image of the surface. This image can be subsequently used to determine surface roughness and other topographical parameters.

Microstructure determination was performed on selected areas of the conventional and additive components. An Olympus BX 61 light microscope was used for this analysis.

2.2 The analysed components and samples

Figure 1a shows the entire component from which the test specimens were prepared for mechanical property testing. The test specimens were prepared from conventional and additive components. Attention was paid to the component's working part, a hexagon coming into contact with the liquid metal, as shown in Figure 1.

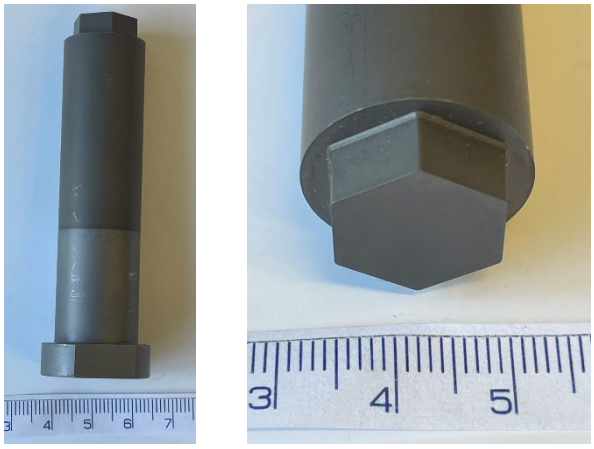

a) the whole component *b) working part detail*
Fig. 1. Example of an aluminium die-casting mould component

In the case of both conventional and additive technology, the analysed components were manufactured from AISI H13 material (W.nr 1.2344). This steel is widely used in hot work tooling applications. It is characterised by good wear resistance at high and low temperatures, good strength at high temperatures, resistance to thermal fatigue, high ductility and toughness. The chemical compositions from the material sheets [15] and [16] for the conventional and powdered AISI H13 steel used to produce the test components are listed in tables 1 and 2.

Table 2.
Chemical composition of the additive H13 tool steel powder provided by the manufacturer [15]

	Cr	**Mo**	**Si**	**V**	**Mn**	**C**
Min	4.75	1.10	0.80	0.80	0.20	0.32
Max	5.50	1.75	1.20	1.20	0.60	0.45

Table 3.
Chemical composition of the conventional H13 tool steel provided by the manufacturer [16]

	Cr	Mo	Si	V	Mn	C
Min	4.70	1.30	0.80	0.80	0.20	0.30
Max	5.50	1.70	1.20	1.20	0.50	0.45

Table 4.
Mechanical properties of H13 tool steel [15], [16]

Materials	Tensile strength– YTS (MPa)	Yield strength – YS (MPa)	Elongation (%)
H13	1770	1450	7.4
H13 powder	1720	1528	4

The production of the components was carried out in several steps at MJF. The aim was to achieve the required mechanical properties and dimensional accuracy. These steps involved:

– SLM additive machining technology
– heat treatment
– machining to final dimensions
– coating.

The selective laser melting (SLM) method was used to produce the additive components, during which the laser gradually melts and bonds the layers of coated powder. The basic parameters of 3D printing are shown in Table 4.

Table 5.
Parameters of 3D print

Layer height	40	µm
Laser power	350	W
Scanning speed	1216	mm/s
Laser path spacing	0,12	Mm

Additive manufacturing using the SLM technology results in rapid heating and subsequent rapid cooling of the material, which can lead to internal stresses. To minimise internal stresses, improve the microstructure and achieve the required hardness (46 ±2 HRC) and high-temperature resistance, heat treatment was performed after 3D printing.

Heat treatment was carried out on both conventional and additive components using the same procedure, involving homogenisation annealing at 1080 °C for 60 minutes, preheating 1 at 650 °C for 15 minutes and preheating 2 at 850 °C for 15 minutes. The austenisation temperature was 1030 °C for 30 minutes with a cooling rate of 28 °C per minute. Further, tempering was carried out at three temperatures: temperature 1 was 570 °C for 3 hours, temperature 2 was 590 °C for 3 hours and temperature 3 was 555 °C for 3 hours. The resulting hardness after heat treatment representing homogenising annealing, quenching and tempering was 46-47 HRC, which is 460-470 HV.

The components were machined to the final dimensions using conventional technologies - turning and milling. In the last stage of the production process, the components were coated. A nanocomposite PVD coating ALWIN® (CrAlSiN), resistant to material sticking to the tool, was applied to the surface. This coating has a high heat resistance of over 1000 °C, making it ideal for use on tools in high-pressure die casting of aluminium alloys.

Four components were selected for the testing of the mechanical properties, as shown in Table 5.

Table 6.
Description of the components selected for the testing of mechanical properties

Samples	Manufacturing method	Pre-test status
C-1	Conventional	127 840 cycles
C-2	Conventional	127 840 cycles
3D-1	SLM	127 840 cycles
3D-2	SLM	127 840 cycles

The primary purpose of the testing was to compare the properties of conventionally and additively manufactured components. For this purpose, we selected two conventionally manufactured components with the designations C-1 and C-2, and two components produced by additive manufacturing with the designations 3D-1 and 3D-2, as seen in Figure 2. The components were subjected to operational testing and were deployed in a die-casting mould. The components were deployed in the mould for 127 840 casting cycles, representing the service life limit of these components. The testing was carried out at the pressure foundry of MOTOR JIKOV Slévárna a.s.

a) Sample C-1 b) Sample C-2 c) Sample 3D-1 d) Sample 3D-2

Fig. 2. Components for test sample production – conventional (a, b) and additive (c, d) manufacturing

As mentioned above, each component was subjected to tensile testing, hardness and roughness measurements, as well as microstructure and porosity determination.

Roughness was analysed at six points on the hexagon of the component, which is the working part that comes into contact with the metal and is subject to the most extensive wear. The measurement points can be seen in Figure 3.

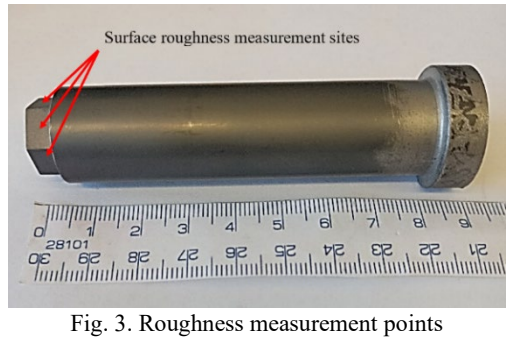

Fig. 3. Roughness measurement points

After completion of the roughness, porosity and hardness measurements, the cut components were used to produce samples for micro-tensile testing, see Figure 4. Four specimens were made from each of the components and subjected to tensile testing. The sample shown in Fig. 4 has a thickness of 1.2 mm.

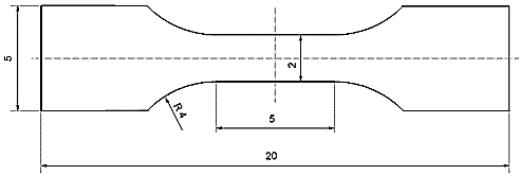

Fig. 4. Diagram of the tensile testing sample (mm)

3. Results and discussion

3.1. Porosity

The porosity measurement also included an assessment of the micro-purity of conventionally and additively manufactured components, due to the likely effect on the material's mechanical properties. Figure 5 shows an example of porosity distribution in a conventional and additive component.

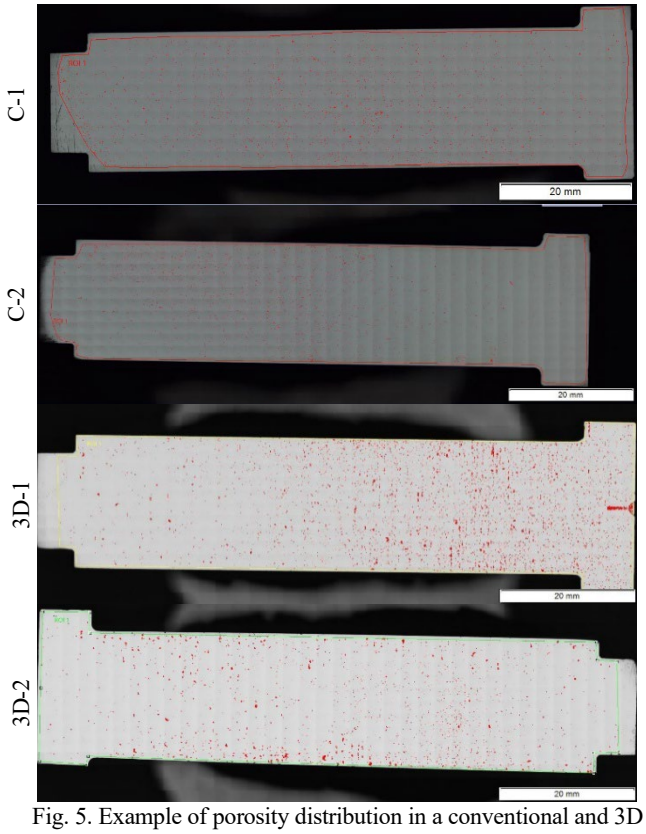

Fig. 5. Example of porosity distribution in a conventional and 3D printed component

Table 6 shows the inclusions values of all the evaluated components. As expected, higher inclusions volumes of 0.25 and 0.30 % were found for the additively manufactured components. Despite this, the inclusions volume in the additively manufactured components was low. The higher inclusions volume was most likely due to the printing parameters. Further testing will be used to optimise the printing parameters to reduce the porosity volume, which will then approach the values of conventionally manufactured components. For conventionally manufactured components, inclusions amounted to 0.03 and 0.04%.

Table 7.
Porosity of the conventional and 3D-printed H13 samples

Conventional samples	**Inclusions (%)**	**3D-printed samples**	Porosity (%)
C-1	0.04	**3D-1**	0.30
C-2	0.03	**3D-2**	0.25

3.2 Tensile test

A tensile test was carried out on the components designated C-1, C-2, 3D-1 and 3D-2. Figure 6 shows the ultimate tensile strength results for the conventional and 3D-printed H13 steel components. The ultimate strength values measured on the worn C-1 and C-2 conventional components were in very good agreement. The measured quantities reached identical mean values with a low standard deviation. This shows that this material exhibited consistent mechanical properties even after operational testing. Component 3D-1 differed by 3.4% compared to the conventional components. Furthermore, the strength limit of component 3D-2 is 15.2% lower than that of theconventional components. The results show that conventional H13 steel retains consistent mechanical properties even after wear. Component 3D-1 has a comparable strength to the conventional material (3.4% variation), while component 3D-2 shows a significantly lower strength (15.2%), indicating the variability of properties in 3D printing. This was most likely influenced by temperature changes or post-treatment.

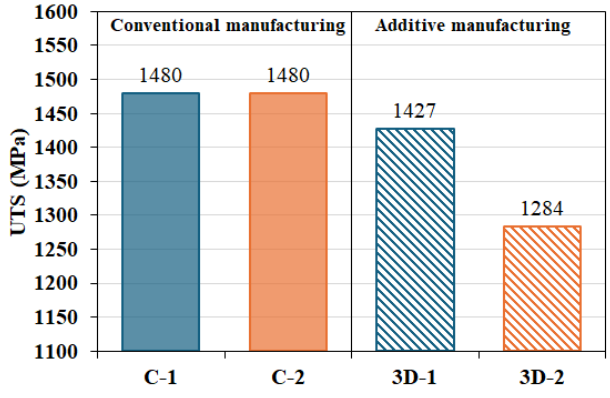

Fig. 6. Comparison of strength limits of the conventional and additive components

The determination of the yield strength is presented in Figure 7. The values measured on worn components C-1 and C-2 of the

conventional material were in very good agreement. Components C-1, C-2 and 3D-1 show very good values. The values measured on component 3D-1 were 3% higher than those measured on the conventionally manufactured components. Furthermore, the yield strength of component 3D-2 was 4.2% lower than for the conventional components. The conventional material shows a stable yield strength even after wear. Component 3D-1 has a slightly higher yield strength of 3 %, indicating good mechanical properties. On the other hand, the yield strength of component 3D-2 is lower by 4.2%, confirming the variability of properties in 3D printing. This is unlikely to have been influenced by temperature changes or subsequent modifications.

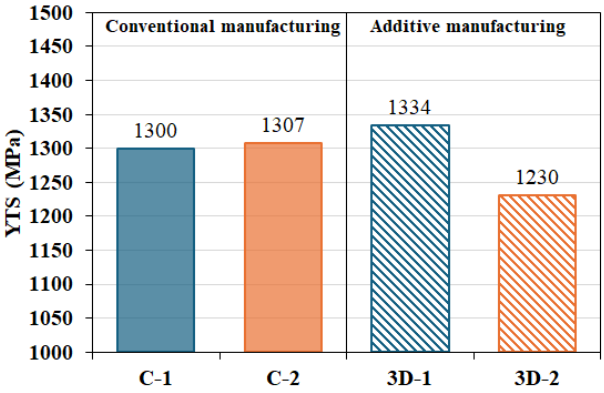

Fig. 7. Comparison of yield strength of conventional and additive components

Figure 8 compares the ductility results of conventional and 3D-printed components. For the conventional components, ductility values of over 20% were measured. The worn 3D-printed components 3D-1 and 3D-2 had ductility values below 1%. Lower ductility is a well-known phenomenon in additive steels, caused by higher porosity, which was also evident in components 3D-1 and 3D-2.

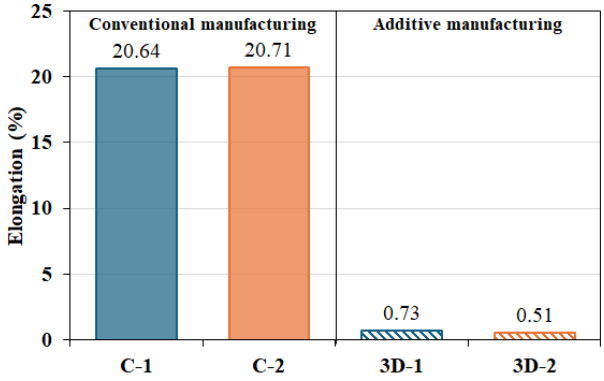

Fig. 8. Comparison of the ductility of conventional and additive components

3.3. Microhardness test

All components' microhardness was measured in 1cm sections. The measurements were taken at points marked 1-9 as seen in Figure 9.

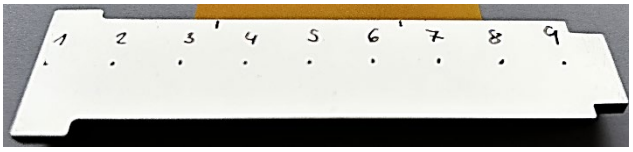

Fig. 9. Hardness measurement points

Figure 10 shows the hardness values of components C-1 and C-2. There is a sharp increase in hardness at points 1 and 2, reaching a peak of 540 HV. Thereafter, the hardness decreases rapidly, stabilising from indentation 3 onwards at approximately 460 HV with minor fluctuations. Overall, the component's hardness stabilises after the fluctuation at indentation 2. The hardness value initially rises sharply to 550 HV. At indentation 3, the value stabilises around 450 HV with slight fluctuations. Components C-1 and C-2 show a significant hardness fluctuation at point 2, indicating that non-standard processing has occurred during the technological processing, namely machining. An increase in hardness values at point 2 can be observed for both components. At the other points, a decrease and subsequent stabilisation of the values at a lower level (C-1 460 HV, C-2 450 HV) can be observed.

Figure 10 shows the trend of hardness values of components 3D-1 and 3D-2. The values of sample 3D-1 initially decrease from 517 HV to 510 HV. Such a small variation can be neglected, and the hardness may be considered constant. The values of sample 3D-2 are in the range of 502-518 HV.

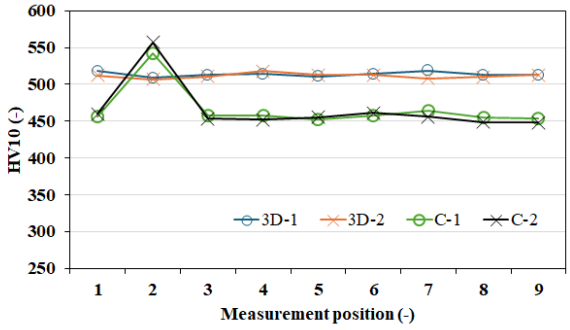

Fig. 10. Comparison of hardness measurements– 3D-1, 3D-2, C-1, C-2

3.4. Surface roughness measurement

The next measurement involves determining the surface roughness of the components. The average surface roughness values are shown in Figure 11.

As can be seen, for the conventional components C-1 and C-2, the measured roughness values were fairly consistent with a low variance of the individual measurement values. The roughness was

measured as 1.1 µm. Different values were found for the additively printed components 3D-1 and 3D-2. A value of 1.2 µm was measured for component 3D-1 and 1.8 µm for component 3D-2. The mean roughness value of the 3D-1 component was at the level of the conventional C-1 and C-2 components, although the higher standard deviation value suggests that roughness varied more on the individual hexagon walls (at the measurement positions). Similarly, the additive component 3D-2 was found to have a roughness approximately 0.6 - 0.7 µm higher than the other components, which may be attributed to the higher wear under the foundry operating conditions. Surface roughness measurements were conducted on the surfaces of components that had been coated with a PVD coating.

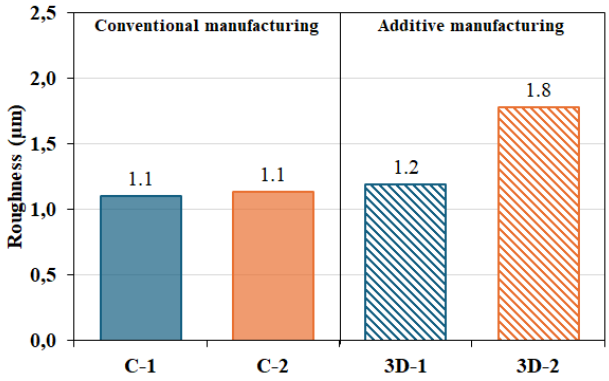

Fig. 11. Roughness of the component's working part

3.5. Light microscopy of conventional and additive components

Light microscopy was performed in three defined areas of the conventional and additive components, as seen in Figure 12, with attention focused on the working part of the components, marked 'crown' in the illustration.

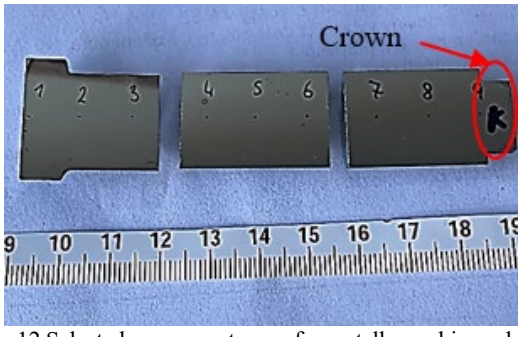

Fig. 12 Selected component areas for metallographic analysis

In Figure 13, microstructures can be observed at the edge of the crown of the conventional components. This type of structure shows that the components have undergone heat treatment and have been subjected to thermal stresses in the operating conditions at the foundry.

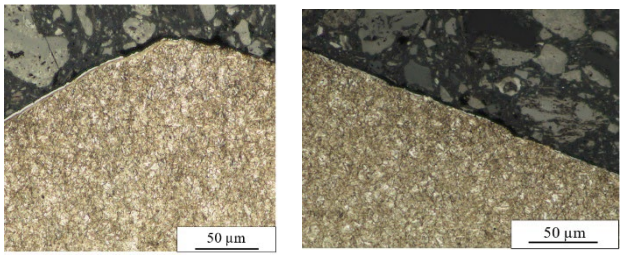

component C-1 *a) component C-2*
Fig. 13. crown– edge, conventional, LM

In Figure 14, microstructures can be observed at the edge of the crown of the additive components. Using light microscopy, layers on the surface can be seen that have been formed by coating with the ALWIN® (CrAlSiN) nanocomposite PVD coating, which provides the tool with resistance to material sticking. These layers are not uniform and range in size from 80 to 200 µm.

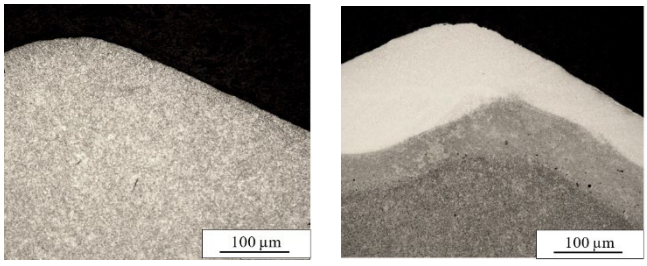

a) component 3D-1 *b) component 3D-2*
Fig. 14. crown– edge, 3D print, LM

Figure 15 shows the microstructures in the centre of the crown of the conventional part. This type of structure indicates that the material was subjected to heat treatment, leading to grain refinement and improvement in mechanical properties such as strength, hardness and resistance to thermal effects.

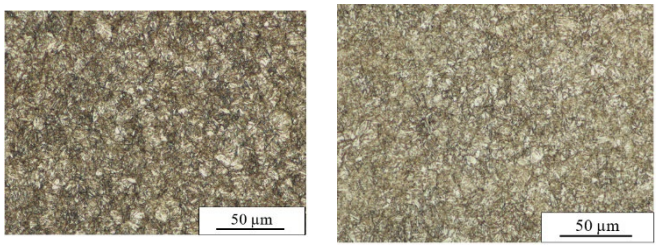

a) component C-1 *b) component C-2*
Fig. 15. crown– edge, conventional, LM

Figure 16 shows the microstructures in the crown centre of the additive components. None of the images of the microstructures preserves the characteristics of additive manufacturing. Thus, without careful description of the components throughout the processes, we cannot tell from the microstructures whether the component is conventional or additive. Traces of additive manufacturing were removed by the heat treatment, during which the material was homogenised.

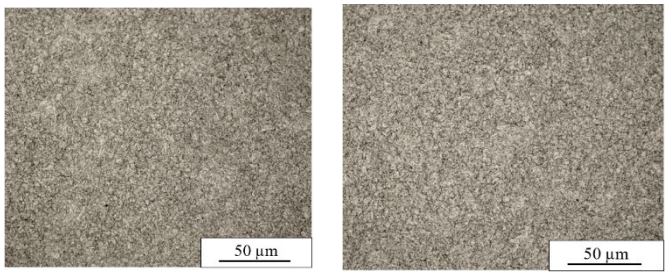

a) component 3D-1 *b) component 3D-2*

Fig. 16. crown – edge, 3D print, LM

4. Conclusions

Our research involved measuring and evaluating the mechanical properties of H13 tool steel components produced by additive and conventional technologies.

- Porosity had a major effect on the ductility of the printed components, with a higher porosity leading to a significant reduction in material ductility. The additively manufactured components generally had higher porosity than the conventional components. Values of 0.25% and 0.30% were measured for the additive components, and 0.03% and 0.04% for the conventional components.
- Tensile tests showed that the yield strength and ultimate tensile strength of the additively manufactured components were comparable to the conventional components despite the larger variance.
- The printed components were found to have a similar yield strength to the conventional material, despite the higher porosity. However, the ductility of the additive components is very low. The measured ductility was 20.6% and 20.7% for the conventional components, while the additive components showed values of 0.5% and 0.7%.
- Material hardness was more stable in the additively manufactured components than in the conventional components. In the conventional components, hardness stabilised after a fluctuation at point 2, indicating the material's relative homogeneity following heat treatment. The hardness values in the conventional components were around 450 HV, while the hardness values in the additive components were around 510 HV. Thus, at the end of the service life of the components, hardness was found to have been affected in the casting machine. The component's hardness after heat treatment was 460-470 HV. The results show that the hardness of the conventional components was 10 HV lower at the end of their service life. On the other hand, the hardness of the additive components was 40 HV higher than the hardness after heat treatment.
- The surface roughness of additively manufactured components showed more variability than conventional components, indicating the importance of adjusting the printing parameters. The average surface roughness was 1.104 and 1.135 µm for the conventional components but 1.186 and 1.775 µm for the additive components.
- Detailed light microscopy showed that the characteristics of additive manufacturing have not been preserved, having been removed by heat treatment resulting in homogenisation. It is impossible to tell from the images of the microstructures whether the component is conventional or additive. The clear visibility of the surface coating, still present at the end of the specified service life, is interesting to note.

Additively manufactured components exhibited inferior mechanical properties and higher porosity compared to conventionally produced parts. Nevertheless, these differences had no negative impact on the specified service life of 120,000 cycles – all tested components reached this threshold without any damage.

Acknowledgements

The paper was funded by the Technology Agency of the Czech Republic within the TREND programme, as part of project Reg. No. FW03010609 “Research and development of shape moulds made of H-13 and DIEVAR for die casting of aluminium alloys in the application of modern technologies of additive production, heat treatment, surface treatment, and numerical simulations”.

References

[1] Véle, F., Ackermann, M., Bittner, V. & Šafka, J. (2021). Influence of selective laser melting technology process parameters on porosity and hardness of AISI H13 tool steel: statistical approach. *Materials.* 14(20), 6052, 1-19. https://doi.org/10.3390/ma14206052.

[2] Nguyen, V.L., Kim, E., Lee, S.-R., Yun, J., Choe, J., Yang, D., Lee, H.-S., Lee, C.-W. & Yu, J.-H. (2018). Evaluation of strain-rate sensitivity of selective laser melted H13 tool steel using nanoindentation tests. *Metals.* 8(8), 589, 1-10. https://doi.org/10.3390/met8080589.

[3] Wang, S., Ning, J., Zhu, L., Yang, Z., Yan, W., Dun, Y., Xue, P., Xu, P., Bose, S. & Bandyopadhyay, A. (2022). Role of porosity defects in metal 3D printing: Formation mechanisms, impacts on properties and mitigation strategies. *Additive Manufacturing*. 60(A), 103256, 1-12. https://doi.org/10.1016/j.addma.2022.103256.

[4] Garcias, J.F., Martins, R. F., Branco, R., Marciniak, Z., Macek, W., Pereira, C. & Santos, C. (2021). Quasistatic and fatigue behavior of an AISI H13 steel obtained by additive manufacturing and conventional method. *Fatigue & Fracture of Engineering Materials & Structures*. 44(1), 3384-3398. https://doi.org/10.1111/ffe.13565.

[5] Lei, F., Wen, T., Yang, F., Wang, J., Fu, J., Yang, H., Wang, J., Ruan, J. & Ji, S. (2022). Microstructures and mechanical properties of H13 tool steel fabricated by selective laser melting. *Materials*. 15(7), 2686, 1-15. https://doi.org/10.3390/ma15072686.

[6] Kim, Y.W., Park, H. & Park, J.M. (2023). High-speed manufacturing-driven strength-ductility improvement of H13 tool steel fabricated by selective laser melting. *Institute of Materials, Minerals and Mining.* 66(5), 582-592. https://doi.org/10.1080/00325899.2023.2241245.

[7] Ahn, W., Park, J., Lee, J., Choe, J., Jung, I., Yu, J. H., Kim, S. & Sung, H. (2018). Correlation between microstructure and mechanical properties of the additive manufactured H13 tool steel. *Korean Journal of Materials Research*. 28(11), 663-670. https://doi.org/10.3740/MRSK.2018.28.11.663.
[8] Bose, A., Reidy, J.P. & Pötschke, J. (2024). Sinter-based additive manufacturing of hardmetals: Review. International *Journal of Refractory Metals and Hard Materials*. 119, 106493, 1-29. https://doi.org/10.1016/j.ijrmhm.2023.106493.
[9] Giarmas, E., Tsakalos, V., Tzimtzimis, E., Kladovasilakis, N., Kostavelis, I., Tzovaras, D. & Tzetzis, D. (2024). Selective laser melting additive manufactured H13 tool steel for aluminum extrusion die component construction. *The International Journal of Advanced Manufacturing Technology*. 133, 4385-4400. https://doi.org/10.1007/s00170-024-14007-7.
[10] Pirinu, A., Primo, T., Del Prete, A., Panella, F.W. & De Pascalis, F. (2022). Mechanical behaviour of AlSi10Mg lattice structures manufactured by the Selective Laser Melting (SLM). *The International Journal of Advanced Manufacturing Technology*. 1651-1680. https://doi.org/10.1007/s00170-022-10390-1.
[11] Hu, Z., Xu, P., Pang, C., Liu, Q., Li, S. & Li, J. (2022). Microstructure and mechanical properties of a high-ductility Al-Zn-Mg-Cu aluminum alloy fabricated by wire and arc additive manufacturing. *Journal of Materials Engineering and Performance*. 31, 6459-6472. https://doi.org/10.1007/s11665-022-06715-6.
[12] Leon, A. & Aghion, E. (2017). Effect of surface roughness on corrosion fatigue performance of AlSi10Mg alloy produced by Selective Laser Melting (SLM). *Materials Characterization.* 131, 188-194. https://doi.org/10.1016/j.matchar.2017.06.029.
[13] Balachandramurthi, A.R., Moverare, J., Dixit, N. & Pederson, R. (2018). Influence of defects and as-built surface roughness on fatigue properties of additively manufactured Alloy 718. *Materials Science and Engineering: A*. 735, 463-474. https://doi.org/10.1016/j.msea.2018.08.072.
[14] Pechlivani, E.M., Melidis, L., Pemas, S., Katakalos, K., Tzovaras, D. & Konstantinidis, A.A. (2023). On the effect of volumetric energy density on the characteristics of 3D-printed metals and alloys. *Metals*. 13(10), 1776, 1-18. https://doi.org/10.3390/met13101776.
[15] SLM SOLUTIONS. (2023). *H13 – Material data sheet*. Retrieved March 18, 2025, from https://www.slm-solutions.com/fileadmin/Content/Powder/MDS/MDS_H13_2023-06_EN.pdf
[16] GNEE. Professional Exported Steel Supplier. (2023). *H13 tool steel*. Retrieved March 25, 2025, from https://cz.coldrolledsteels.com/info/h13-tool-steels-88814121.html